*Article*

# In Situ Reduction of Silver Nanoparticles on the Plasma-Induced Chitosan Grafted Polylactic Acid Nonwoven Fabrics for Improvement of Antibacterial Activity

Yu Ren [1], Tingyue Fan [1], Xiaona Wang [1], Yongyin Guan [2], Long Zhou [2], Li Cui [2], Meixian Li [1,*] and Guangyu Zhang [1,*]

[1] School of Textile and Clothing, Nantong University, Nantong 226019, China; ren.y@ntu.edu.cn (Y.R.); fty4869@163.com (T.F.); wxn20082021@163.com (X.W.)

[2] Huzhou Zhongshi Technology Co., Ltd., Xin Feng Ming Group, Huzhou 313000, China; gyy@xfmgroup.com (Y.G.); zl@xfmgroup.com (L.Z.); cl@xfmgroup.com (L.C.)

[*] Correspondence: lmx321@ntu.edu.cn (M.L.); zgyu85@ntu.edu.cn (G.Z.)

**Abstract:** An eco-friendly approach for improvement of antibacterial properties of polylactic acid (PLA) nonwoven fabrics was obtained by in situ reduction of silver nanoparticles (Ag NPs) on dielectric barrier discharge (DBD) plasma-induced chitosan grafted (DBD-CS-Ag NPs) PLA nonwoven fabrics. The surface morphology, surface element composition and the chemical state of silver of the PLA surfaces after the treatment were evaluated through scanning electron microscopy (SEM), energy dispersive X-ray (EDX), Fourier transform infrared spectroscopy (FTIR), X-ray photoelectron spectroscopy (XPS) and X-ray diffraction (XRD), respectively. The antibacterial activity of DBD-CS-Ag NPs treated PLA against *Escherichia coli (E. coli)* and *Staphylococcus aureus (S. aureus)* was tested. The uniform dispersion of silver nanoparticles on the DBD-CS-Ag NPs treated PLA surface were confirmed by SEM images. The results of XPS and XRD showed that the concentration of silver element on the surface of PLA nonwoven fabrics was significantly improved after DBD-CS-Ag NPs treatment. The DBD-CS-Ag NPs treated PLA nonwoven fabrics also exhibited excellent antibacterial properties.

**Keywords:** polylactic acid; plasma-induced graft; chitosan; silver nanoparticles; antibacterial performance

## 1. Introduction

As the world's oil resources are increasingly exhausted and the environmental pollution is becoming more and more serious, the search for renewable resources has gradually attracted people's attention. Polylactic acid (PLA) has been regarded as the most promising sustainable and biodegradable fiber to replace conventional polyethylene terephthalate (PET) polyester fiber in textile products. It is also widely used in medical and health, agriculture and forestry protection, and packaging materials due to its good physical and mechanical properties, excellent biocompatibility, and natural degradation [1–3]. However, there are still some disadvantages in the properties of PLA materials, such as high inertia, poor hydrophilicity and difficulty to react with other substances, which greatly limit the further development of PLA in the field of biomedical functional materials [4,5].

At present, studies on surface modification of PLA have been widely performed, including copolymerization [6], blending [7], crosslinking [8] and so on. Among these methods, dielectric barrier discharge (DBD) plasma has attracted much more attention due to the reduction of the complicated vacuum system, energy saving, and the stable and reliable treatment effect [9–11]. Plasma treatment only acts on the superficial layer of the materials, which can significantly improve the hydrophilicity, adhesion, and dyeing properties of the material surface without damaging the matrix properties [12–15]. Ren et al. [16] used atmospheric pressure DBD plasma treatment to improve the surface wettability of PLA nonwovens. With the prolongation of the treatment time, micro and nano structures

were formed on the surface of PLA, resulting in sharp decrease of water contact angle which showed super hydrophilicity.

Cheng et al. [17] applied the nitrogen-based DBD jet system to treat the PLA film. The results showed that the cell growth on PLA surface was enhanced using the DBD plasma treatment. Sauerbier et al. [18] investigated whether the DBD plasma treatment could activate the surface of PLA-based wood-plastic composites and improve the coating capabilities. Kudryavtseva et al. [19] obtained the bioactive PLA based scaffolds with hyaluronic acid via atmospheric pressure plasma assisted modification method. It was shown that atmospheric pressure plasma treatment led to the changes of surface chemical composition of the PLA-based scaffolds increasing long-term hydrophilicity of the scaffold surface.

Silver nanoparticles (Ag NPs) have attracted considerable attention due to their antibacterial activities and broad-spectrum bioactivities [20–25]. Traditionally, chemical reduction is a common method to prepare nano silver-containing antibacterial textiles. In brief, silver ions are adsorbed on the textiles, followed by the addition of reducing agent to reduce silver ions to Ag NPs [26,27]. However, reducing agent causes environmental pollution. Therefore, in-situ reduction method without reducing agent takes place of the traditional chemical reduction method. In this method, textiles are functionalized to adsorb silver ions and in situ reduced to Ag NPs without any reducing agents. It not only simplifies the process, but also reduces the production cost [28,29].

Chitosan is one of the most popular natural cationic polymers, which is obtained by deacetylation of chitin from crustaceans, insects and other sources. Chitosan is a biodegradable, nontoxic, antibacterial, and biocompatible polymer and is widely used in food processing, biomedical, water purification, daily chemical industry, agriculture and other fields [30,31]. In recent years, chitosan has been widely used in the hygienic antibacterial textiles [32–35]. Also, chitosan has been reported to improve fabric properties such as dye ability and anti-shrinkage. Ren et al. [36] treated ultrahigh molecular weight polyethylene fibers by the combined treatment of DBD plasma and chitosan coatings for the improvement of surface wettability, dye ability and adhesion properties.

In this work, an eco-friendly approach for improvement of antibacterial properties of PLA nonwoven fabrics was obtained by in situ reduction of Ag NPs on the plasma-induced chitosan grafted PLA nonwoven fabrics. PLA nonwoven fabrics were pretreated by atmospheric pressure argon DBD plasma to improve its surface reactivity. Then, chitosan was grafted on the surface of PLA as a stabilizer and a reducing agent, and Ag NPs were adsorbed and in situ reduced on the surface of chitosan grafted PLA nonwoven fabrics. The surface morphology, chemical composition, and chemical state of silver were analyzed. The antibacterial properties were investigated according to GB/T 20944.3-2008 (China) and GB/T 20944.3-2008 (China), using the inhibition zone method and the shake flask method, respectively.

## 2. Materials and Methods

### 2.1. Materials

PLA spunbonded nonwoven fabrics with an areal density of 70 $g/m^2$ and thickness of about 0.25 mm were provided by Shenzhen Shengdefu Materials Technology Co., Ltd. (Shenzhen, China). The PLA nonwoven fabrics were washed with deionized water for 10 min to remove water-soluble impurities, followed by ultrasonic cleaning in absolute ethanol for 20 min to remove organic impurities, and then the samples were dried at 60 °C for 2 h in an oven.

Chitosan (viscosity average molecular weight $5 \times 10^5$, deacetylation degree 90%) was purchased from Jinshuiqiao Biotechnology Co., Ltd., (Yantai, China). Acetic acid, $AgNO_3$, $NaH_2PO_4$, $KH_2PO_4$, and NaOH were purchased from Runjie Chemical Reagent Co., Ltd. (Shanghai, China). All reagents used in this work were analytically pure. *Escherichia coli (E. coil)* (ATCC 8099), *Staphylococcus aureus (S. aureus)* (ATCC 6538), nutrient broth, and nutrient agar were obtained from Weidi Biotechnology Co., Ltd., (Shanghai, China).

### 2.2. Preparation of Chitosan Grafted PLA Nonwoven Fabrics

Atmospheric pressure DBD equipment (APP-350, fabricated by Institute of Micro-electronics of Chinese Academy of Science, Beijing, China) was utilized for the plasma treatment of the PLA nonwoven fabrics. The PLA nonwoven fabrics were placed between two parallel plates with about 2 mm distance of the gap between the quartz glass layer and the ground electrode and treated by argon (1 L/min) plasma for 90 s. The input of 200 V, 50 Hz was given to the high voltage step-up transformer from the main power supply.

The desired amount of chitosan was dissolved in 2% *w/v* acetic acid aqueous solution to obtain 1% *w/v* concentration of chitosan solution and stirred for 10 h at the room temperature. The control and freshly DBD plasma pretreated PLA nonwoven fabrics were separately immersed into the chitosan solution using a liquor ratio of 40:1 at 50 °C for 60 min in the constant-temperature water bath (Spring Instrument Co., Ltd., Shanghai, China). Subsequently, the samples were washed with deionized water to remove physically adhered chitosan solution followed by drying at 45 °C in oven for 2 h.

### 2.3. Preparation of Chitosan Grafted PLA/Ag NPs Nonwoven Fabrics

Chitosan grafted PLA (CS-PLA) nonwoven fabrics and DBD plasma treated chitosan grafted PLA (DBD-CS-PLA) were immersed in $AgNO_3$ solution (400 mL,1 g/L) with a liquor ratio of 1:40 for 60 min at room temperature, respectively. After being loaded Ag NPs, the samples were then washed in deionized water and dried at 45 °C for 2 h in oven.

### 2.4. Surface Morphology Observation

To determine the color changes of the PLA nonwoven fabrics after Ag NPs loading, the surface topography of the PLA nonwoven fabrics was observed by an optical microscope and a field emission scanning electron microscope (FE-SEM, HITACHI Group SU8020, Tokyo, Japan) with a VANTANGE 100 energy dispersive X-ray (EDX) spectrometer, respectively. Samples were sputtered with gold under vacuum prior to SEM observation, and the SEM images were recorded with secondary electrons with the magnification of 10,000 under an accelerating voltage of 3.0 kV.

### 2.5. Surface Chemical Composition Analysis

X-ray photoelectron spectroscopy (XPS) analysis was utilized to determine the changes of the chemical component of the treated PLA nonwoven fabrics using the ESCALAB250 X-ray photoelectron spectrometer system (Thermo-VG Scientific Co., Ltd., London, UK). The X-ray source was Cu K$\alpha$ (1486.6 eV) and the operating power was 150 W. The XPS analysis was performed under $10^{-7}$–$10^{-8}$ Pa and the photo emitted electrons were collected at a take-off angle of 45°.

The PLA nonwoven fabrics with or without treatment were investigated by the attenuated total reflection-fourier transform infrared spectroscope (ATR-FTIR, PerkinElmer Spectrum Two, PerkinElmer, Inc., Fremont, CA, USA). The ATR-FTIR spectra were investigated between the wavenumber from 4000 to 650 cm$^{-1}$ with 64 scans at a resolution of 4 cm$^{-1}$.

### 2.6. X-ray Diffraction (XRD) Pattern

The crystallography of the PLA nonwoven fabrics with or without treatment were characterized via XRD (Bruker AXS company D8 Advance, Berlin, Germany) by using a Cu K$\alpha$ X-ray light source with 40 kV voltage and the scanning range was from 5° to 80°.

### 2.7. Antibacterial Activity Test

The inhibition zone method and the shaking flask method are used to conduct qualitative and quantitative tests on the antibacterial properties of the samples, respectively.

The antibacterial activity of CS-Ag NPs-PLA and DBD-CS-Ag NPs-PLA against *E. coli* and *S. aureus* was tested according to GB/T 20944.3-2008 (China) using the inhibition zone method [37]. The samples were cut into a circle with a diameter of about 15 mm, and wrap the round sample with a piece of paper for sterilization at 126 °C under 103 kPa pressure

for 15 min. The cultured suspension was diluted to $1 \times 10^5$ CFU/mL with PBS buffer, and 1 mL suspension was evenly smeared on agar medium. Then the samples were attached to the culture medium respectively, and put into the biochemical incubator for 24 h at 37 °C.

The antibacterial activity of CS-PLA, DBD-PLA, CS-Ag NPs-PLA and DBD-CS-Ag NPs-PLA against *Escherichia coli (E. coli)* and *Staphylococcus aureus (S. aureus)* was tested according to GB/T 20944.3-2008 (China) using the shake flask method [38]. 0.75 g of the pristine PLA sample was cut into pieces of about 0.5 cm $\times$ 0.5 cm size, and immersed in a flask containing 70 mL of 0.3 mM phosphate buffer saline medium with a concentration of $1 \times 10^5$–$4 \times 10^5$ CFU/mL. The flask was then shaken on a rotary shaker at 24 °C with 150 rpm for 18 h. 1 mL of the solution was taken from each of the incubated samples, diluted and dispensed onto agar plates. All plates were incubated at 37 °C for 24 h and the formed colonies were counted.

## 3. Results and Discussion

### 3.1. Infrared Spectra

An ATR-FTIR spectrum was employed to investigate the changes in chemical structure of the PLA nonwoven fabrics after the treatment. Figure 1 shows the ATR-FTIR spectra of the chitosan, PLA nonwoven fabrics and DBD-CS-Ag NPs treated PLA. As shown in Figure 1b the untreated PLA exhibited peaks at 1750 cm$^{-1}$ attributed to C=O stretching vibration, 3002 cm$^{-1}$ attributed to –CH asymmetric stretching vibration, 1384 cm$^{-1}$ attributed to –CH$_3$ symmetric deformation vibration. It was found in Figure 1c that the new peaks appeared in the ATR-FTIR spectra of the DBD-CS-Ag NPs treated PLA fabrics. The new absorption band 1590 and 1540 cm$^{-1}$ (attributed to C=O stretching vibration of amide I and N–H bending vibration, respectively) [39] and a broad region 3000–3470 cm$^{-1}$ (contributed to –OH, –NH or NH$_2$ stretching vibrations) were observed [36,40]. The presence of new peaks proves the introduction of chitosan (Figure 1a) onto the PLA fabrics through the chitosan and DBD-CS combined treatment.
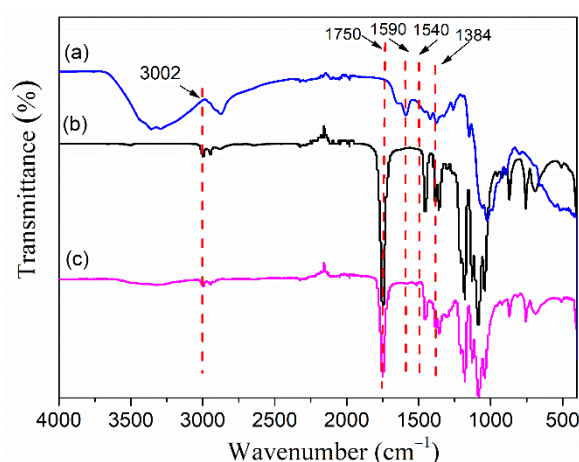


**Figure 1.** FTIR spectra of (**a**) chitosan; (**b**) control PLA nonwoven fabrics; (**c**) DBD-CS-Ag NPs treated fabric.

### 3.2. XRD Analysis

In order to verify the chemical state of Ag NPs on the surface of PLA nonwoven fabrics, XRD tests were carried out on PLA nonwoven fabrics with or without surface treatment, and the results are shown in Figure 2. It can be seen from Figure 2 that compared with the XRD spectra of PLA nonwoven fabrics, the diffraction peaks of the treated samples at the positions of 2θ at 38.3°, 44.5°, 64.5°, and 77.6° are consistent with (111), (200), (220) and (311) crystal planes of cubic crystal system. The peak intensity of the DBD-CS-Ag NPs-PLA nonwoven fabrics is higher than that of CS-Ag NPs-PLA nonwoven fabrics. This fully proves that DBD plasma treatment and chitosan grafting create a synergy effect on

silver ion absorption and its reduction, which is obviously better than the samples only grafted with chitosan [41].
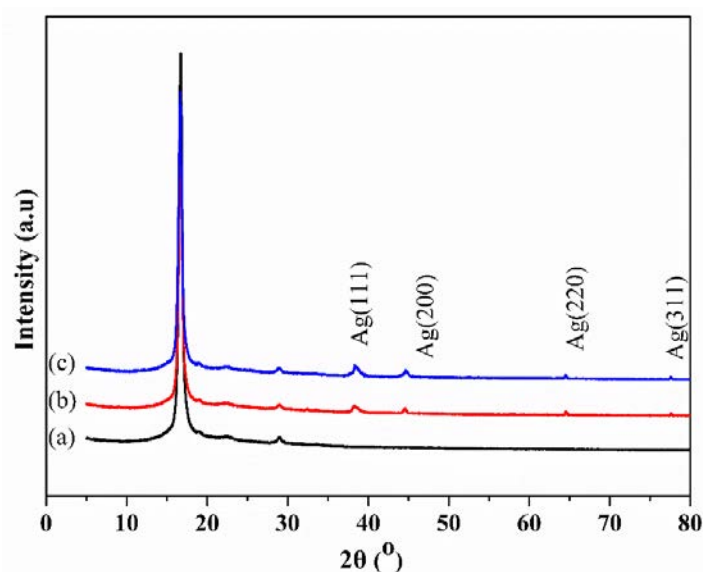


**Figure 2.** XRD survey scan of PLA nonwoven fabrics: (**a**) control; (**b**) CS-Ag NPs treated; (**c**) DBD-CS-Ag NPs treated.

*3.3. Surface Appearance and Morphology Analysis of PLA Based Nonwoven Fabrics*

After treating with Ag NPs, the whiteness of the PLA nonwoven fabrics changed. The appearance of PLA based nonwoven fabrics with or without treatment were shown in Figure 3. As shown in Figure 3a the untreated PLA nonwoven fabrics have a white appearance. Due to the optical properties of Ag NPs, when coating with Ag NPs the color of the fabric will become brown, the higher Ag NPs content, the darker of the fabric. After treating with Ag NPs, CS-Ag NPs-PLA nonwoven fabrics and DBD-CS-Ag NPs-PLA nonwoven fabrics (Figure 3b,c) turn light brown and dark brown, respectively. The results can also confirm that the surface of DBD-CS-Ag NPs-PLA nonwoven fabrics adsorbs more Ag NPs than that of CS-Ag NPs-PLA nonwoven fabrics.
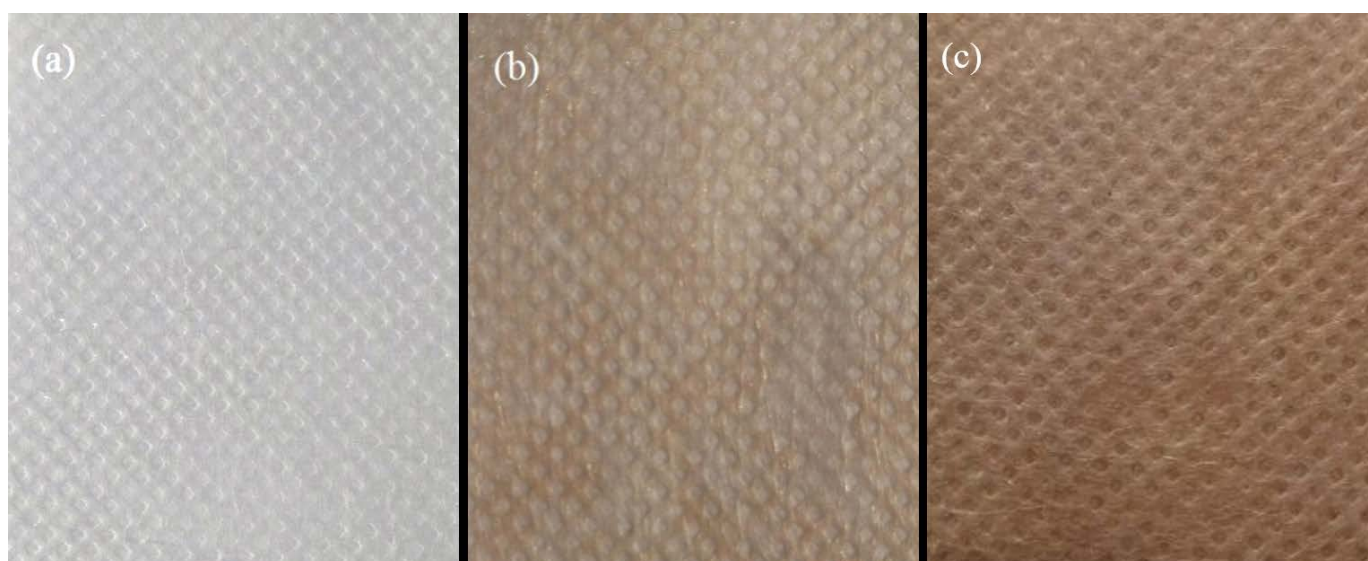


**Figure 3.** Optical photographs of PLA nonwoven fabrics: (**a**) original PLA (control); (**b**) CS-Ag NPs PLA; (**c**) DBD CS-Ag NPs-PLA.

The surface morphology of PLA based nonwoven fabrics was observed by FE-SEM. It can be seen from Figure 4 that the original PLA nonwoven fabrics have a smooth and clean surface, and almost no impurities are adsorbed on the surface. On the other hand, Ag NPs appeared on the surface of treated PLA nonwoven fabrics with diameter of 100 nm. The content of Ag NPs on the surface of CS-Ag NPs-PLA nonwoven fabrics is low and the distribution is uneven, whereas that of DBD-CS-Ag NPs-PLA nonwoven fabrics significantly increase and the distribution is much more uniform. This indicates that after DBD plasma treatment, silver ions are more easily absorbed from silver nitrate solution onto the surface of CS-PLA nonwoven fabrics and then in situ reduced to form Ag NPs, leading to high loading amount and uniform dispersion of Ag NPs.
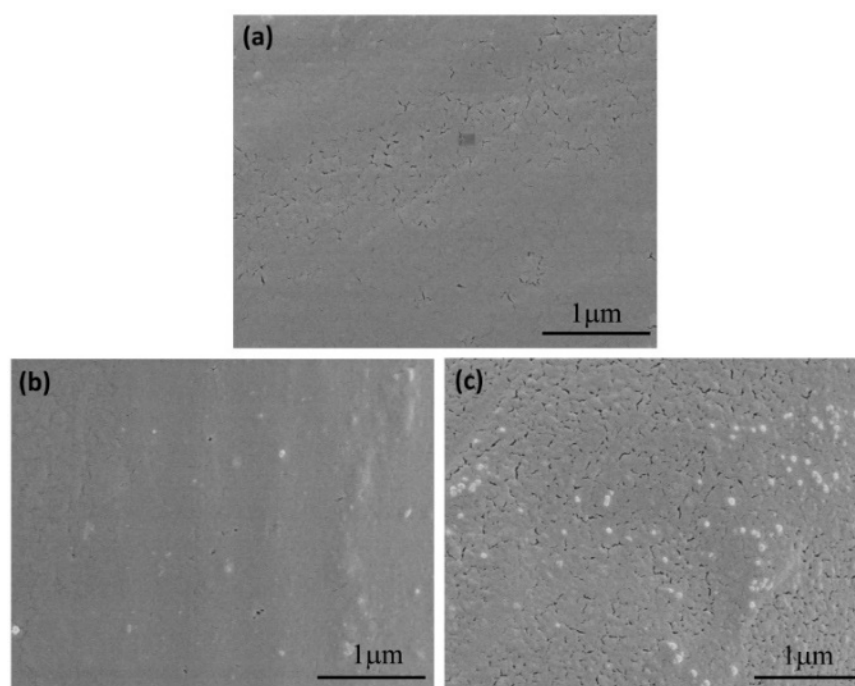


**Figure 4.** SEM images of surface topography of PLA nonwoven fabrics (**a**) control; (**b**) CS-Ag NPs-PLA; (**c**) DBD-CS-Ag NPs-PLA.

### 3.4. Analysis of Surface Chemical Composition

In order to further clarify the loading of Ag NPs on PLA nonwoven fabrics, EDX and XPS were carried out on different samples which, respectively, reflected the changes of element types and contents on the surface of materials. The EDX and XPS spectra of the samples are shown in Figures 5 and 6, respectively.

By comparing the spectra of Figure 5a–c, it can be seen that there are only two peaks of C and O in the original sample of PLA nonwoven fabrics, while there are C, O, and Ag peaks in the samples which were treated with chitosan and Ag NPs. The silver content of CS-Ag NPs-PLA nonwoven fabrics is 0.31%, while that of DBD-CS-Ag NPs-PLA nonwoven fabrics increases to 1.01%. The reason may be that a large number of active groups were introduced to the surface of the samples after plasma pretreatment, which increases the reaction activity of the sample surface and absorbs more Ag NPs on the surface.

It can be clearly seen from Figure 6 that the original PLA nonwoven fabrics only have C1s peak at 285 eV and O1s peak at 532 eV, while the treated PLA nonwoven fabrics have N1s peak at 400 eV and Ag3d peak at 368 eV and 374 eV. Moreover, the surface Ag3d peak of DBD-CS-Ag NPs-PLA nonwoven fabrics is obviously stronger than that of CS-Ag NPs-PLA nonwoven fabrics. Combined with Table 1, it can be seen that the surface of CS-Ag NPs-PLA only contains 0.41% Ag, while that of CS-Ag NPs-PLA contains 3.91% Ag. This shows that DBD plasma treatment can greatly increase the content of Ag on the surface of CS-Ag NPs-PLA nonwoven fabrics.
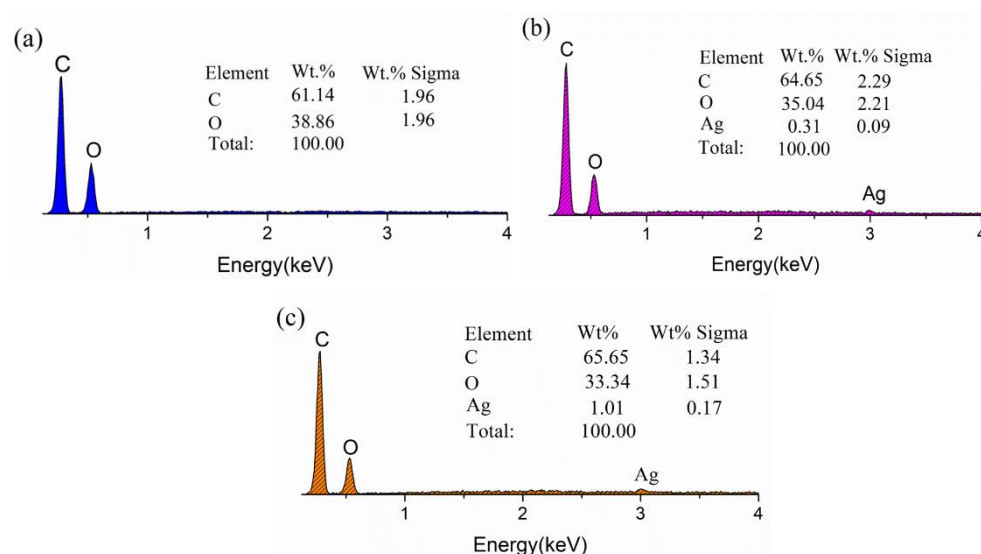
**Figure 5.** EDX spectra of PLA nonwoven fabrics: (**a**) control; (**b**) CS-Ag NPs treated; (**c**) DBD-CS-Ag NPs treated.
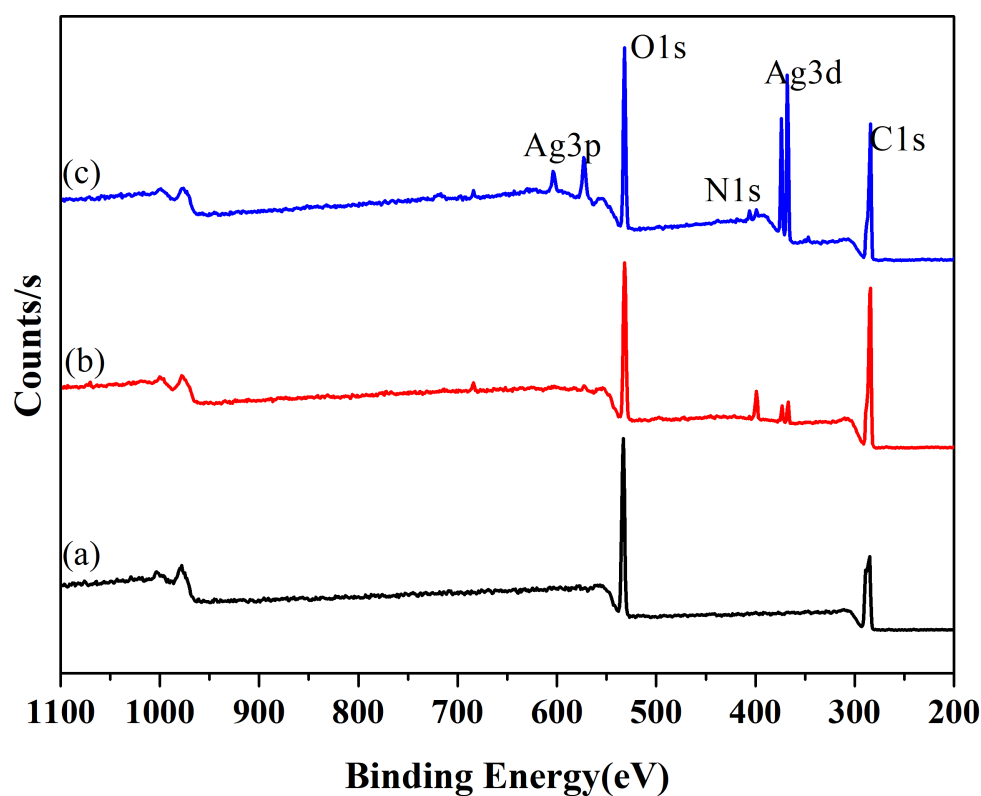


**Figure 6.** XPS survey scan of PLA nonwoven fabrics: (**a**) control; (**b**) CS-Ag NPs treated; (**c**) DBD-CS-Ag NPs treated.

**Table 1.** Relative surface chemical composition determined by XPS for the control and the Ag NPs loaded PLA fabrics.

| Samples | Chemical Composition (%) | | | |
|---|---|---|---|---|
| | C1s | O1s | N1s | Ag |
| Original PLA (Control) | 62.18 | 37.82 | - | - |
| CS-Ag NPs treated | 68.55 | 24.08 | 6.97 | 0.41 |
| DBD-CS-Ag NPs treated | 64.16 | 28.9 | 3.04 | 3.91 |

In addition, the Ag3d spectrum of DBD-CS-Ag NPs-PLA nonwoven fabrics is shown in Figure 7. There is a strong Ag3d peak at 368 eV, which is basically consistent with the binding energy peak of silver (368.2 eV). At the same time, the energy level difference between $Ag3d_{3/2}$ and $Ag3d_{5/2}$ is 6 eV, which is completely consistent with the standard binding energy of elemental silver [42,43]. This basically proves the existence of elemental silver on the surface of DBD-CS-Ag NPs-PLA nonwoven fabrics.
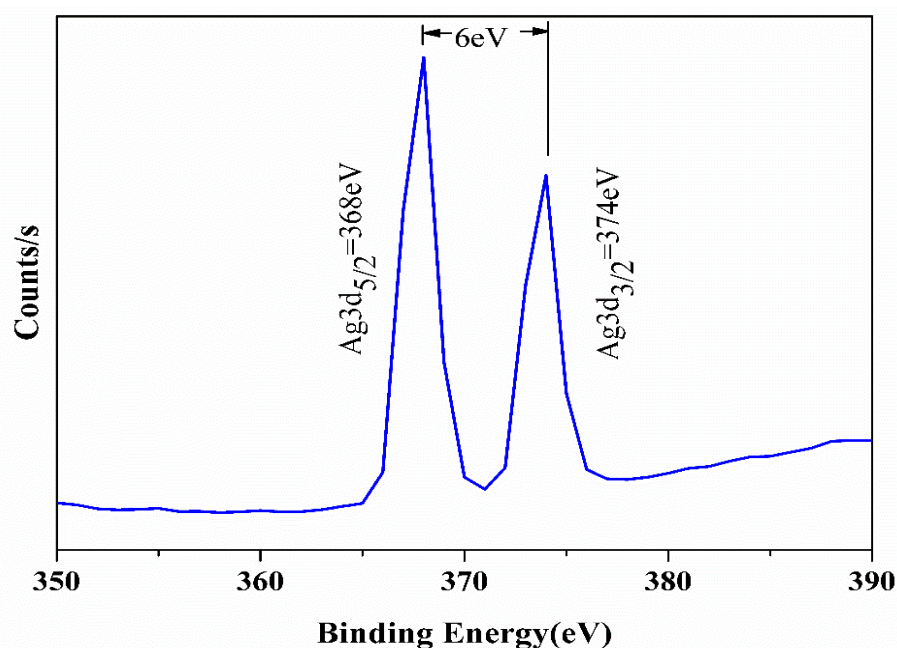


**Figure 7.** Ag3d XPS peak of DBD-CS-Ag NPs treated PLA nonwoven fabrics.

*3.5. Antibacterial Activity*

The antibacterial activity tests of treated PLA fabrics were carried out against *S. aureus* and *E. coli*. Figure 8a,b are the antibacterial effect diagram of CS-Ag NPs-PLA nonwoven fabrics against *E. coli* and *S. aureus*, while Figure 8c,d shows that of DBD-CS-Ag NPs-PLA nonwoven fabrics against *E. coli* and *S. aureus*. Generally, the larger the inhibition zone, the better the antibacterial effect of the fabric. Around the control fabric, there was a dense population of bacterial colonies which revealed no antibacterial activity. On the contrary, clear inhibition zones could be distinctly observed around treated samples, indicating that the two kinds of samples have certain antibacterial properties to *E. coli* and *S. aureus*, and the antibacterial property to *S. aureus* is better than *E. coli*. Meanwhile, as it is shown in Figure 8, the antibacterial effect of DBD-CS-Ag NPs-PLA nonwovens on *E. coli* and *S. aureus* is better than that of CS-Ag NPs-PLA nonwoven fabrics.

*S. aureus* and *E. coli* representatives were selected to determine the antibacterial activity of the treated PLA fabric and the result was shown in Table 2. After treated with chitosan, both CS treated and DBD-CS treated PLA fabrics have a certain degree of antibacterial activity. As chitosan was a biologic cationic polyelectrolyte with weak antibacterial properties, the antibacterial activity of chitosan treated PLA fabric for both the *S. aureus* and *E. coil* no more than 50%. However, the antibacterial activity of Ag NPs treated PLA fabrics shows a significant improvement. The antibacterial activity of the DBD-CS-Ag NPs-PLA nonwovens fabrics to *E. coli* and *S. aureus* can reach up to 99.99%. The improvement of the antibacterial properties of DBD-CS-Ag NPs-PLA nonwovens fabrics indicates that the DBD plasma treatment facilitates the deposition of Ag NPs on the PLA surfaces.
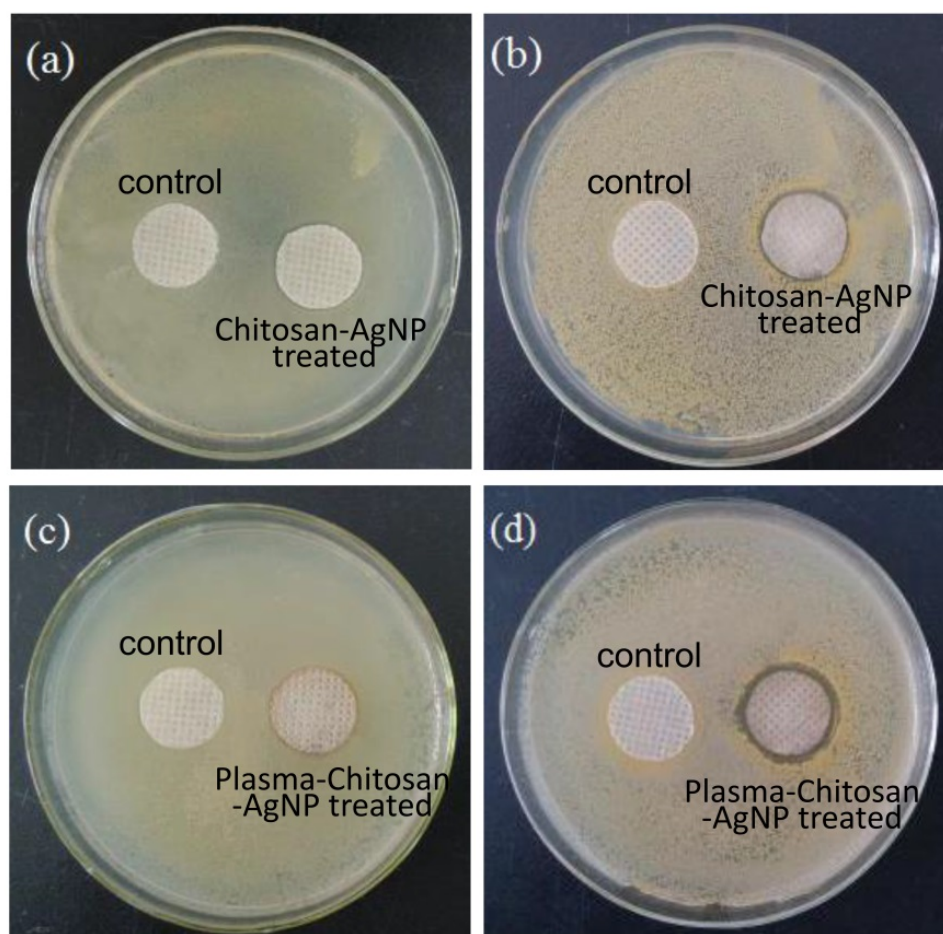
**Figure 8.** Photographs of inhibition zone of PLA nonwoven fabrics: (**a**) CS-Ag NPs treated (*E. coil*); (**b**) CS-Ag NPs treated (*S. aureus*); (**c**) DBD-CS-Ag NPs treated (*E. coil*); (**d**) DBD-CS-Ag NPs treated (*S. aureus*).

**Table 2.** Reduction percent of bacteria according to the GB/T 20944.3-2008 standard method.

| Samples | Strains | 24 h (CFU) | R% |
|---|---|---|---|
| Control | *E. coli* | $2.1 \times 10^4$ | - |
| | *S. aureus* | $1.3 \times 10^4$ | - |
| CS treated | *E. coli* | $1.6 \times 10^4$ | 23.8 |
| | *S. aureus* | $0.8 \times 10^4$ | 30.7 |
| DBD-CS treated | *E. coli* | $1.2 \times 10^4$ | 42.8 |
| | *S. aureus* | $6.6 \times 10^3$ | 49.2 |
| CS-Ag NPs treated | *E. coli* | $5.9 \times 10^3$ | 71.9 |
| | *S. aureus* | $2.4 \times 10^3$ | 81.5 |
| DBD-CS-Ag NPs treated | *E. coli* | <10 | 99.99 |
| | *S. aureus* | <10 | 99.99 |

*3.6. Mechanism of Silver Particles Absorption on PLA Nonwoven Fabrics*

The possible mechanism of in-situ formation of Ag NPs on the surface of chitosan treated PLA nonwoven fabrics is shown in Figure 9, which is divided into three steps. Firstly, PLA nonwoven fabrics were treated by plasma. Non-treated PLA has bulky methyl groups, ester groups as well as methyl groups, and only few polar groups such as hydroxyl group and carboxyl group can be found in the end group. Plasma treatment can introduce more hydroxyl and carboxyl groups on the surface of PLA, which are beneficial to the chitosan grafting [36]. In the second step, the hydroxyl and carboxyl groups in PLA fabrics can interact with amino or hydroxyl groups in chitosan molecules through hydrogen bonds

and covalent bond to enhance the adhesion between the PLA nonwoven fabrics surface and chitosan molecules [44]. The third step is the interaction between CS-PLA nonwoven fabrics and silver ion solution. The amino and hydroxyl groups in chitosan have a stable coordination effect on silver ions, therefore, silver ions can be easily adsorbed on the surface of the fabric [45]. At the same time, silver ions can be effectively in situ reduced to Ag NPs by the hydroxyl groups of chitosan.
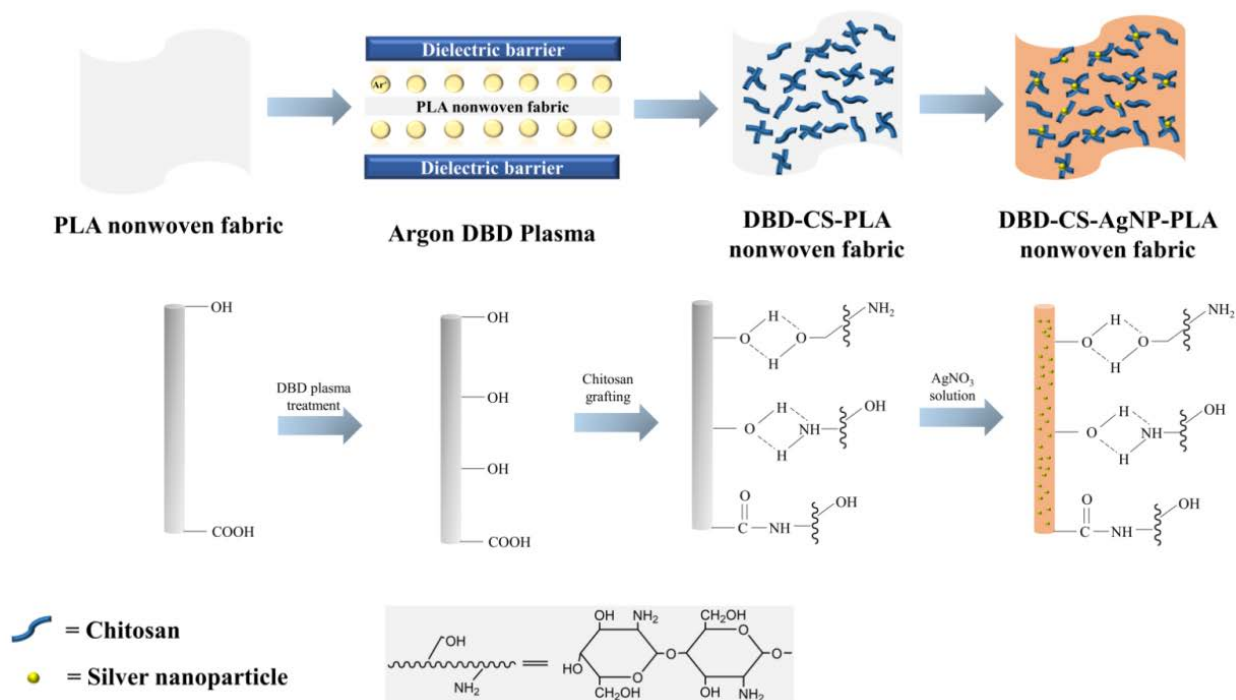


**Figure 9.** The possible mechanism of chitosan deposition on PLA nonwoven fabrics pretreated by plasma and the original flavor reduction of silver nanoparticles.

Meanwhile, compared with the CS-Ag NPs-PLA nonwoven fabrics, more silver element deposited on the DBD-CS-Ag NPs-PLA nonwovens fabrics. This is due to the fact that the surface of PLA nonwoven fabrics is roughened and a large number of reactive functional groups are produced which promotes the chemical binding of chitosan macromolecules and makes chitosan evenly coated on the material surface. When it contacts with silver nitrate solution, the chitosan on the surface of PLA nonwoven fabrics will in-situ reduce silver ions to Ag NPs which effectively enhance the antibacterial property of PLA nonwoven fabrics.

## 4. Conclusions

In this work PLA nonwoven fabrics were grafted with chitosan after the DBD plasma treatment. Ag NPs were in situ reduced on the chitosan grafted PLA surfaces as a stabilizer and a reducing agent for improvement the antibacterial properties. SEM observation showed that the Ag NPs with 100 nm diameter were evenly distributed on the surface of PLA nonwovens. The results of EDX and XPS showed that the silver element on the surface of PLA nonwovens was significantly improved after plasma treatment combined with chitosan grafting and Ag NPs adsorption. In addition, the XRD results fully proved that the plasma treatment combined with chitosan grafting could successfully reduce silver ions to Ag NPs on the surface of PLA nonwovens. The results of antibacterial circle test exhibited that the antibacterial circle radius of DBD-CS-Ag NPs-PLA nonwovens to *E. coli* and *S. aureus* is significantly larger than that of CS-Ag NPs-PLA nonwovens, indicating that the combination of DBD plasma and chitosan grafting is more effective in improving the antibacterial property of PLA nonwovens. Moreover, the antibacterial rate

of PLA nonwovens to *E. coli* and *S. aureus* increased to 99.99% after DBD plasma treatment combining with chitosan grafting and Ag NPs.

**Author Contributions:** Conceptualization, Y.R. and T.F.; data curation, Y.R., Y.G., L.Z., M.L. and G.Z.; formal analysis, M.L.; investigation, X.W., Y.G. and L.C.; methodology, X.W., L.Z. and L.C.; project administration, G.Z.; supervision, G.Z.; writing—original draft, Y.R., T.F. and M.L. All authors have read and agreed to the published version of the manuscript.

**Institutional Review Board Statement:** Not applicable.

**Informed Consent Statement:** Not applicable.

**Data Availability Statement:** Data is contained within the article.

**Conflicts of Interest:** The authors declare no conflict of interest.

## References

1. Slepička, P.; Michaljaničová, I.; Kasálková, N.S.; Kolská, Z.; Rimpelová, S.; Ruml, T.; Švorčík, V. Poly-l—lactic acid modified by etching and grafting with gold nanoparticles. *J. Mater. Sci.* **2013**, *48*, 5871–5879. [CrossRef]
2. Nampoothiri, K.M.; Nair, N.R.; John, R.P. An overview of the recent developments in polylactide (PLA) research. *Bioresour. Technol.* **2010**, *101*, 8493–8501. [CrossRef]
3. Sui, L.; Zhang, B.S.; Wang, J.; Cai, A.N. Polymerization of PEDOT/PSS/chitosan-coated electrodes for electrochemical bio-sensing. *Coatings* **2017**, *7*, 96. [CrossRef]
4. Murariu, M.; Dubois, P. PLA composites: From production to properties. *Adv. Drug Deliv. Rev.* **2016**, *107*, 17–46. [CrossRef]
5. Armentano, I.; Bitinis, N.; Fortunati, E.; Mattioli, S.; Rescignano, N.; Verdejo, R.; Lopez-Manchado, M.A.; Kenny, J.M. Multifunctional nanostructured PLA materials for packaging and tissue engineering. *Prog. Polym. Sci.* **2013**, *38*, 1720–1747. [CrossRef]
6. Manju, P.; Krishnan, P.S.G.; Kumar, N.S. Chemical modifications of PLA through copolymerization. *Int. J. Polym. Anal. Charact.* **2020**, *25*, 634–648. [CrossRef]
7. MariaBeatrice, C.; Norma, M.; Sara, R.; Stefano, F.; Francesca, S.; Andrea, L. Compatibilization of poly(lactic acid) (PLA)/plasticized cellulose acetate extruded blends through the addition of reactively extruded comb copolymers. *Molecules* **2021**, *26*, 2006. [CrossRef]
8. Melania, B.; Katarina, B.; Przemysław, K. Crosslinking of polylactide by high energy irradiation and photo-curing. *Molecules* **2020**, *25*, 4919. [CrossRef]
9. Ren, Y.; Wang, C.; Qiu, Y. Influence of aramid fiber moisture regain during atmospheric plasma treatment on aging of treatment effects on surface wettability and bonding strength to epoxy. *Appl. Surf. Sci.* **2007**, *253*, 9283–9289. [CrossRef]
10. Ren, Y.; Wang, C.; Qiu, Y. Aging of surface properties of ultra high modulus polyethylene fibers treated with He/O$_2$ atmospheric pressure plasma jet. *Surf. Coat. Technol.* **2007**, *202*, 2670–2676. [CrossRef]
11. Wang, C.X.; Ren, Y.; Lv, J.C.; Zhou, Q.Q.; Ma, Z.P.; Qi, Z.M.; Chen, J.Y.; Liu, G.L.; Gao, D.W.; Lu, Z.Q.; et al. In situ synthesis of silver nanoparticles on the cotton fabrics modified by plasma induced vapor phase graft polymerization of acrylic acid for durable multifunction. *Appl. Surf. Sci.* **2017**, *396*, 1840–1848. [CrossRef]
12. Jelil, R.A. A review of low-temperature plasma treatment of textile materials. *J. Mater. Sci.* **2015**, *50*, 5913–5943. [CrossRef]
13. Jordavilaplana, A.; Fombuena, V.; Garciagarcia, D.; Samper, M.D.; Sancheznacher, L. Surface modification of polylactic acid (PLA) by air atmospheric plasma treatment. *Eur. Polym. J.* **2014**, *58*, 23–33. [CrossRef]
14. Salem, T.; Uhlmann, S.; Nitschke, M.; Calvimontes, A.; Hund, R.-D.; Simon, F. Modification of plasma pre-treated PET fabrics with poly-DADMAC and its surface activity towards acid dyes. *Prog. Org. Coat.* **2011**, *72*, 168–174. [CrossRef]
15. Shahidi, S.; Ghoranneviss, M.; Wiener, J. Improving synthetic and natural dyeability of polyester fabrics by dielectric barrier discharge. *J. Plast. Film Sheeting* **2015**, *31*, 286–308. [CrossRef]
16. Ren, Y.; Xu, L.; Wang, C.; Wang, X.; Ding, Z.; Chen, Y. Effect of dielectric barrier discharge treatment on surface nanostructure and wettability of polylactic acid (PLA) nonwoven fabrics. *Appl. Surf. Sci.* **2017**, *426*, 612–621. [CrossRef]
17. Cheng, K.; Chang, C.; Yang, Y.; Liao, G.; Liu, C.; Wu, J. Enhancement of cell growth on honeycomb-structured polylactide surface using atmospheric-pressure plasma jet modification. *Appl. Surf. Sci.* **2017**, *394*, 534–542. [CrossRef]
18. Sauerbier, P.; Köhler, R.; Renner, G.; Militz, H. Surface activation of polylactic acid-based wood-plastic composite by atmospheric pressure plasma treatment. *Materials* **2020**, *13*, 4673. [CrossRef]
19. Kudryavtseva, V.; Stankevich, K.; Gudima, A.; Kibler, E.; Zhukov, Y.; Bolbasov, E.; Malashicheva, A.; Zhuravlev, M.; Riabov, V.; Liu, T.; et al. Atmospheric pressure plasma assisted immobilization of hyaluronic acid on tissue engineering PLA-based scaffolds and its effect on primary human macrophages. *Mater. Des.* **2017**, *127*, 261–271. [CrossRef]

20. Khodadadi, B.; Bordbar, M.; Yeganeh-Faal, A.; Nasrollahzadeh, M. Green synthesis of Ag nanoparticles/clinoptilolite using Vaccinium macrocarpon fruit extract and its excellent catalytic activity for reduction of organic dyes. *J. Alloys Compd.* **2017**, *719*, 82–88. [CrossRef]

21. Wan, C.; Jiao, Y.; Sun, Q.; Li, J. Preparation, characterization, and antibacterial properties of silver nanoparticles embedded into cellulose aerogels. *Polym. Compos.* **2016**, *37*, 1137–1142. [CrossRef]

22. Sun, B.; Hua, B.; Ji, X.; Shi, Y.; Zhou, Z.; Wang, Q.; Zhu, M. Preparation of silver nanoparticles with hydrophobic surface and their polyester based nanocomposite fibres with excellent antibacterial properties. *Mater. Res. Innov.* **2014**, *18*, 869–874. [CrossRef]

23. Jin, L.S.; Nyoung, H.D.; Ji-Hoi, M.; Wan-Kyu, K.; Bok, L.J.; Soo, B.M.; Woong, P.S.; Eun, K.J.; Hyun, L.D.; Eun-Cheol, K.; et al. Electrospun chitosan nanofibers with controlled levels of silver nanoparticles. Preparation, characterization and antibacterial activity. *Carbohydr. Polym.* **2014**, *111*, 530–537. [CrossRef]

24. Yildiz, A.; Bayramol, D.V.; Atav, R.; Ağirgan, A.Ö.; Kurç, M.A.; Ergünay, U.; Mayer, C.; Hadimani, R.L. Synthesis and characterization of Fe$_3$O$_4$@Cs@Ag nanocomposite and its use in the production of magnetic and antibacterial nanofibrous membranes. *Appl. Surf. Sci.* **2020**, *521*, 146332. [CrossRef]

25. Xu, Q.; Li, R.; Shen, L.; Xu, W.; Wang, J.; Jiang, Q.; Zhang, L.; Fu, F.; Fu, Y.; Liu, X. Enhancing the surface affinity with silver nano-particles for antibacterial cotton fabric by coating carboxymethyl chitosan and L-cysteine. *Appl. Surf. Sci.* **2019**, *497*, 143673. [CrossRef]

26. El-Shishtawy, R.M.; Asiri, A.M.; Abdelwahed, N.A.M.; Al-Otaibi, M.M. In situ production of silver nanoparticle on cotton fabric and its antimicrobial evaluation. *Cellulose* **2011**, *18*, 75–82. [CrossRef]

27. Yazdanshenas, M.E.; Shateri-Khalilabad, M. The effect of alkali pre-treatment on formation and adsorption of silver nanoparticles on cotton surface. *Fibers Polym.* **2012**, *13*, 1170–1178. [CrossRef]

28. Xu, L.Y.; Lai, Y.L.; Liu, L.; Yang, L.L.; Guo, Y.; Chang, X.J.; Shi, J.J.; Zhang, R.Y.; Yu, J.Y. The effect of plasma electron temperature on the surface properties of super-hydrophobic cotton fabrics. *Coatings* **2020**, *10*, 160. [CrossRef]

29. Montazer, M.; Malekzadeh, S.B. Electrospun antibacterial nylon nanofibers through in situ synthesis of nanosilver: Preparation and characteristics. *J. Polym. Res.* **2012**, *19*, 9980. [CrossRef]

30. Aider, M. Chitosan application for active bio-based films production and potential in the food industry: Review. *LWT-Food Sci. Technol.* **2010**, *43*, 837–842. [CrossRef]

31. Dai, J.M.; Luo, Y.; Nie, D.; Jin, J.H.; Yang, S.L.; Li, G.; Yang, Y.M.; Zhang, W. pH/photothermal dual-responsive drug delivery and synergistic chemo-photothermal therapy by novel porous carbon nanofibers. *Chem. Eng. J.* **2020**, *397*, 125402. [CrossRef]

32. Alaswad, S.O.; Lakshmi, K.B.; Sudha, P.N.; Gomathi, T.; Arunachalam, P. Toxic heavy metal cadmium removal using chitosan and polypropylene based fiber composite. *Int. J. Biol. Macromol.* **2020**, *164*, 1809–1824. [CrossRef]

33. Xufei, L.; Junzhi, S.; Yangli, C.; Yan, L.; Fang, L. Antibacterial properties of chitosan chloride-graphene oxide composites modified quartz sand filter media in water treatment. *Int. J. Biol. Macromol.* **2019**, *121*, 760–773. [CrossRef]

34. Preethi, S.; Abarna, K.; Nithyasri, M.; Kishore, P.; Deepika, K.; Ranjithkumar, R.; Bhuvaneshwari, V.; Bharathi, D. Synthesis and characterization of chitosan/zinc oxide nanocomposite for antibacterial activity onto cotton fabrics and dye degradation applications. *Int. J. Biol. Macromol.* **2020**, *164*, 2779–2787. [CrossRef] [PubMed]

35. Bajpai, S.K.; Thomas, V.; Bajpai, M. Novel strategy for synthesis of ZnO microparticles loaded cotton fabrics and investigation of their antibacterial properties. *J. Eng. Fibers Fabr.* **2011**, *6*, 73–81. [CrossRef]

36. Ren, Y.; Ding, Z.; Wang, C.; Zang, C.; Zhang, Y.; Xu, L. Influence of DBD plasma pretreatment on the deposition of chitosan onto UHMWPE fiber surfaces for improvement of adhesion and dyeing properties. *Appl. Surf. Sci.* **2017**, *396*, 1571–1579. [CrossRef]

37. Wei, D.; Dong, C.; Liu, J.; Zhang, Z.; Lu, Z. A novel cyclic polysiloxane linked by guanidyl groups used as flame retardant and antimicrobial agent on cotton fabrics. *Fibers Polym.* **2019**, *20*, 1340–1346. [CrossRef]

38. Guangyu, Z.; Dao, W.; Jiawei, Y.; Yao, X.; Wenyan, G.; Chuanfeng, Z. Study on the photocatalytic and antibacterial properties of TiO$_2$ nanoparticles-coated cotton fabrics. *Materials* **2019**, *12*, 2010. [CrossRef]

39. Debnath, T.; Islam, M.S.; Hoque, S.; Haque, P.; Rahman, M.M. Preparation and characterization of chitosan grafted poly(lactic acid) films for biomedical composites. *J. Polym. Eng.* **2020**, *40*, 333–341. [CrossRef]

40. Pandiyaraj, K.N.; Ferraria, A.M.; Rego, A.M.B.d.; Deshmukh, R.R.; Su, P.-G.; Halleluyah, J.M.; Halim, A.S. Low-pressure plasma enhanced immobilization of chitosan on low-density polyethylene for bio-medical applications. *Appl. Surf. Sci.* **2015**, *328*, 1–12. [CrossRef]

41. Sutton, A.; Franc, G.; Kakkar, A. Silver metal nanoparticles: Facile dendrimer-assisted size-controlled synthesis and selective catalytic reduction of chloronitrobenzenes. *J. Polym. Sci. Part A Polym. Chem.* **2009**, *47*, 4482–4493. [CrossRef]

42. Kaspar, T.C.; Droubay, T.; Chambers, S.A.; Bagus, P.S. Spectroscopic evidence for Ag (III) in highly oxidized silver films by X-ray photoelectron spectroscopy. *J. Phys. Chem. C* **2010**, *114*, 21562–21571. [CrossRef]

43. Liao, Y.; Wang, Y.; Feng, X.; Wang, W.; Xu, F.; Zhang, L. Antibacterial surfaces through dopamine functionalization and silver nanoparticle immobilization. *Mater. Chem. Phys.* **2010**, *121*, 534–540. [CrossRef]

44. Biswas, D.P.; O'Brien-Simpson, N.M.; Reynolds, E.C.; O'Connor, A.J.; Tran, P.A. Comparative study of novel in situ decorated porous chitosan-selenium scaffolds and porous chitosan-silver scaffolds towards antimicrobial wound dressing application. *J. Colloid Interface Sci.* **2018**, *515*, 78–91. [CrossRef]

45. Murugadoss, A.; Chattopadhyay, A. A 'green' chitosan–silver nanoparticle composite as a heterogeneous as well asmicro-heterogeneous catalyst. *Nanotechnology* **2008**, *19*, 015603. [CrossRef] [PubMed]